

1
2
3
4
5
6
7
8
9
10
11
12
13
14
15
16
17

Relating degradation of pharmaceutical active ingredients in a stream network to degradation in water-sediment simulation tests

Mark Honti¹, Fabian Bischoff², Andreas Moser², Christian Stamm², Sándor Baranya³, and Kathrin Fenner^{2,4}

¹MTA-BME Water Research Group, Hungarian Academy of Sciences, Budapest, Hungary.

²Department of Environmental Chemistry, EAWAG Swiss Federal Institute of Aquatic Science and Technology, Dübendorf, Switzerland.

³Department of Hydraulic and Water Resources Engineering, Budapest University of Technology and Economics, Budapest, Hungary.

⁴Chemistry Department, University of Zürich, Zürich, Switzerland

Key Points:

- Biotransformation of pharmaceuticals takes place in small to medium streams.
- OECD 308 tests underestimate pharmaceutical biotransformation rates yet overestimate total degradation in the Rhine basin.
- Assessment of pharmaceutical persistence from measured river fluxes is conditional on precise emission and removal data.

Corresponding author: Mark Honti, mark.honti@gmail.com

18 **Abstract**

19 Many pharmaceuticals inevitably end up in surface waters, exerting unwanted biological
20 activity in non-target organisms. This effect is confined by the compound's environmental
21 persistence. Regulatory laboratory simulation tests are used in persistence assessment and
22 exposure modelling. While doubt has been expressed about the usefulness of laboratory-
23 derived persistence indicators under field conditions, these remain the only inputs for
24 chemical fate models due to difficulties of measuring persistence in situ, especially at large
25 scales. To improve understanding about relationships between laboratory experiments and
26 the environmental fate in streams, we developed a mathematical model of biodegradation
27 in stream networks and combined it with in-stream monitoring data to (i) test if persis-
28 tence could be evaluated from field data, (ii) check if persistence extracted from laboratory
29 tests applied in the field, and (iii) locate hot-spots of biodegradation in a large river basin.
30 The model describes partitioning, and particle settling and resuspension, and is structurally
31 compatible with those applied for evaluating laboratory simulation tests. Application to
32 the Rhine river basin suggests that biotransformation rate constants extracted from lab-
33 oratory tests underestimate those in the field, yet the percentage of biotransformation in
34 the Rhine basin is less than in the laboratory tests due effective biotransformation being
35 limited to small and medium-sized streams. In conclusion, our data show that biotransfor-
36 mation rates can accurately predicted if (i) monitoring is performed across a wide range in
37 stream order, and (ii) precise estimates for consumption and removal rates at wastewater
38 treatment plants are known.

39 **1 Introduction**

40 The production, use and disposal of plant protection products, human and veteri-
41 nary pharmaceuticals, biocides, and industrial chemicals inevitably lead to the pollution
42 of surface water bodies due to direct use in the environment, accidental spills, or incom-
43 plete removal during wastewater treatment. Since most of these substances intentionally
44 exhibit biological activity, they bear the potential to harm aquatic ecosystems. Although
45 continuous emissions can make chemicals seem pseudo-persistent, the actual levels of
46 their pollution and its duration after emission has ceased is determined by (real) persis-
47 tence, i.e., how fast the pollutant is removed by biological and chemical degradation pro-
48 cesses [Boethling *et al.*, 2009]. For surface water systems, the most important transfor-

49 mation processes determining persistence include chemical hydrolysis, direct and indi-
50 rect photo-transformation, and microbial biotransformation. The speed and extent of these
51 transformation processes determine the persistence of chemicals and therefore play an im-
52 portant role in the regulatory risk assessment of chemicals. In regulatory frameworks, a
53 compound's persistence is often assessed in laboratory-based test systems using a so-called
54 tiered approach (i.e., if the compound fails to be degraded in the rather simple, yet strin-
55 gent lower-tier tests, its degradation is studied in increasingly complex, yet environmen-
56 tally more realistic higher-tier test systems; cf. REACH [ECHA], Canadian Guideline for
57 Determining Environmental Chemistry and Fate of Pesticides [Agriculture Canada, Envi-
58 ronment Canada, and Department of Fisheries and Oceans 1987], EPA OPPTS Guidelines
59 [US EPA]).

60 The higher-tier test systems, also called simulation tests, are meant as closer repre-
61 sentations of the real environment compared to biodegradability and hydrolysis tests, yet
62 they exhibit superior reproducibility and lower costs compared to tests carried out in the
63 field. As a consequence, they form the backbone of regulatory assessment in cases when
64 simpler tests cannot prove the lack of persistence in the environment, which, due to their
65 rather complex chemical structure, is the case for most water-relevant organic micropol-
66 lutants such as pesticides and pharmaceuticals. For the evaluation of the microbial bio-
67 transformation of chemicals in surface water systems, two OECD testing guidelines are
68 relevant: The OECD 308 guideline ("*Aerobic and Anaerobic Transformation in Aquatic*
69 *Sediment Systems*"), which targets transformation at the water-sediment interface, and the
70 OECD 309 guideline ("*Aerobic mineralization in surface water – Simulation biodegrada-*
71 *tion test*"), which assesses transformation in the pelagic water body (with or without a cer-
72 tain amount of suspended sediment). Simulation tests have a double purpose: they should
73 provide a standardised platform to get comparable information about the biotransforma-
74 tion of chemicals in freshwater systems for regulatory persistence assessment, and to yield
75 relevant environmental half-lives for exposure modelling.

76 The usage of simulation test results in exposure modelling presumes that persistence
77 parameters and indicators are transferable to real catchments. However, parameter transfer
78 from laboratory to the field has been shown to be challenging even for abiotic processes.
79 Catchments typically show lower abiotic process rates than the targeted laboratory systems
80 [Pačes, 1983; Swoboda-Colberg and Drever, 1993; Liu et al., 2013; Wen and Li, 2018],
81 with different physical conditions and heterogeneity as main suspects for the systematic

82 difference. The persistence of organic micropollutants is governed by biological processes
83 on the top of abiotic conditions, suggesting a more complex relationship. However, the
84 extrapolation of biotransformation rates from laboratory to the field has not been system-
85 atically addressed yet. This gap is of high regulatory relevance, therefore we focus on the
86 usefulness of laboratory-derived persistence indicators in exposure modelling inside a large
87 river basin.

88 Since its introduction, various issues with OECD 308 have been reported and dis-
89 cussed [*Davis et al.*, 2005; *Ericson*, 2007; *Ericson et al.*, 2013; *Radke and Maier*, 2014].
90 A main point of criticism was the concern about the relevance of the test conditions with
91 regard to degradation in actual surface water bodies. OECD 308 is carried out in a dark
92 and stagnant environment, where 2-3 cm of settled – and mostly anaerobic – sediment lies
93 under a 6-9 cm shallow water column. Due to the complete lack of mixing, there is no
94 suspended sediment and mass transport is limited to molecular diffusion. The low water-
95 sediment ratio, the shallow depth of the water column, and stagnant conditions were listed
96 as atypical for most surface water bodies affected by pharmaceutical emissions. These
97 issues do not preclude using these tests for the regulatory assessment of persistence, yet
98 they question their relevance for field conditions.

99 The OECD 309 system is criticised for being (i) vaguely standardised due to the nu-
100 merous allowed variants (pelagic/non-pelagic, light/dark), and (ii) a very expensive form
101 of hydrolysis and sorption test due to the typically very low level of biotransformation ob-
102 served in such systems – probably due to the low provision of organic matter and degrader
103 biomass.

104 Scientific literature reports on other types of persistence experiments that seek to
105 more closely mimic the situation in the natural environment, such as flumes [*Kunkel and*
106 *Radke*, 2008; *Li et al.*, 2015], limnocorrals [*Solomon et al.*, 1985; *Liber et al.*, 1997], and
107 mass balance experiments in the field [*Tixier et al.*, 2002, 2003; *Fono et al.*, 2006; *Huntscha*
108 *et al.*, 2008], yet these have not penetrated into regulatory practice yet.

109 Criticism against simulation studies can be distilled into issues about system com-
110 plexity and definition: On the one hand, a simulation test is too complex to interpret its
111 results directly. Biotransformation usually interferes with phase transfer and formation of
112 non-extractable residues so that the extraction of degradation half-lives requires inverse
113 modelling [*Honti and Fenner*, 2015]. On the other hand, the test systems are overly sim-

114 plistic and too strictly standardised compared to the complexity and variability of the real
115 environment. The majority of flowing waters with their complex sediment dynamics is
116 neither represented well by the stirred-suspended nor the stagnant experimental types.
117 While there is a scientific consensus that experimental persistence does not directly project
118 into persistence in the environment, to this day we still lack methods that could relate
119 half-lives in specific laboratory systems to half-lives in the field. Presumably, the wide
120 spectrum of physical conditions in surface water systems suggest that such methods should
121 rely on certain physics-independent indicators of persistence, which could then be related
122 to the specific environmental conditions. Yet common experimental persistence indicators
123 are all specific to the experimental system.

124 The k'_{bio} concept [Honti *et al.*, 2016] disentangles biotransformation from phase
125 transfer and bioavailability in OECD 308 and OECD 309 type test systems, which allows
126 converting half-lives between different compartments and experimental types. However,
127 the model of Honti *et al.* [2016] is limited to closed experimental systems and therefore is
128 not suited to simulate behaviour under field conditions.

129 Therefore, we extended this model to streams to allow for a direct comparison with
130 monitoring results for pharmaceuticals along the river Rhine measured by Ruff *et al.* [2015]
131 and address the following research questions:

- 132 1. Can persistence of chemicals in a stream network be evaluated from field data?
- 133 2. Can experimental half-lives measured in the laboratory be used in the field?
- 134 3. Where along a stream network is biotransformation the most intense?

135 We present a new model that describes the biotransformation of pharmaceuticals in
136 the riverine environment in analogy with the spiralling concept developed for nutrient cy-
137 cling in streams [Newbold *et al.*, 1981; Ensign and Doyle, 2006]. Nutrients pass through
138 various abiotic and biotic stages along their travel downstream, which can be concep-
139 tualised as an extension of the local nutrient cycle into a spatial spiral. Micropollutants
140 undergo rather similar processes: the cycle built of phase partitioning pathways taking
141 place in closed simulation tests, such as the OECD 308 and 309, develops into a spiral in
142 streams, which in turn leaves its imprint on the observable behaviour of the pollutant in
143 the field. We formulate a simple first-order model structure that contains phase partition-
144 ing and downstream transport in an integrated manner. It is assumed that emissions and

145 flow are both permanent (continuous and constant), which is reasonable for pharmaceuti-
146 cals. Loss processes other than biotransformation (phototransformation, hydrolysis, etc.)
147 are not considered in the model, yet we show how they can be included.

148 The present study approaches modelling micropollutant biotransformation in stream
149 networks from the regulatory side. This approach requires a coverable data demand to re-
150 duce the uncertainty of calibration, careful consideration of sediment dynamics to ensure
151 a realistic description of partitioning, and a structural compatibility with models of OECD
152 308 (beyond taking the lab-derived half-lives) for facilitating parameter comparison be-
153 tween the laboratory systems and the field.

154 There are already models simulating the fate and transport of micropollutants in
155 (European) stream networks, but none of them fulfils the above requirements completely.
156 The GREAT-ER model [Feijtel *et al.*, 1997; Koormann *et al.*, 2006] determines PEC values
157 in individual stream segments using a stochastic approach. GREAT-ER solves analytical
158 versions of transport equations and uses seasonal scenarios instead of time-dynamics. The
159 STREAM-EU model [Lindim *et al.*, 2016] simulates transport in all media, not only sur-
160 face waters, combining high spatial resolution and time-dynamics, resulting in a highly
161 complex mathematical structure and a corresponding high data demand. The WATER
162 model [Trapp and Matthies, 1998] describes in-stream transport, yet sediment dynamics
163 are controlled by parameters unrelated to both hydraulic properties of the reach and sed-
164 iment quality. The TOXRIV model [Trapp and Matthies, 1998] does not assume steady
165 states and hence requires detailed hydraulic and water quality data. In summary, struc-
166 tural compatibility to OECD 308 is missing from all above models, partitioning is over-
167 simplified in certain models, and some are just too complex compared to data availability
168 in large catchments.

169 **2 Methods**

170 The new model is based on river reaches, where partitioning and transformation in
171 an equilibrium state are described as functions of the physical properties of the reach and
172 the physico-chemical properties of the compound. The pollutant's behaviour in an entire
173 catchment is simulated by connecting multiple stream reaches following the topology of
174 the stream network.

175 The Rhine catchment upstream of the Dutch-German border is presented as a case-
176 study. The stream network is built up from reaches and basic physical properties were as-
177 signed based on the CCM2 river and catchment database (EU JRC, <http://ccm.jrc.ec.europa.eu/>).
178 The model is calibrated for 7 active pharmaceutical ingredients (APIs) using emission data
179 from the CrossWater project [Moser *et al.*, 2018; Ingold *et al.*, 2018], estimated excretion
180 and WWTP removal data from Singer *et al.* [2016], and pharmaceutical flux measurements
181 by Ruff *et al.* [2015]. Model results are analysed both in terms of parameter values and
182 spatial distribution. Calibrated biotransformation parameters are compared to values ob-
183 tained from regulatory studies. Calculated degradation of APIs in different parts of the
184 stream network are analysed to reveal potential hotspots of degradation.

185 Out of the seven APIs, four are kept anonymous and will be referred to here as
186 API6, API8, API9, and API13, as their confidential OECD 308 experimental dossiers were
187 kindly provided by the German Environment Agency [Fenner *et al.*, 2016]. Their coding
188 here is not consecutive in order to keep the original codes of Fenner *et al.* [2016]. The re-
189 maining three APIs lack associated experimental results, they are carbamazepine (CMZ),
190 sitagliptin (SIG), and trimethoprim (TTP).

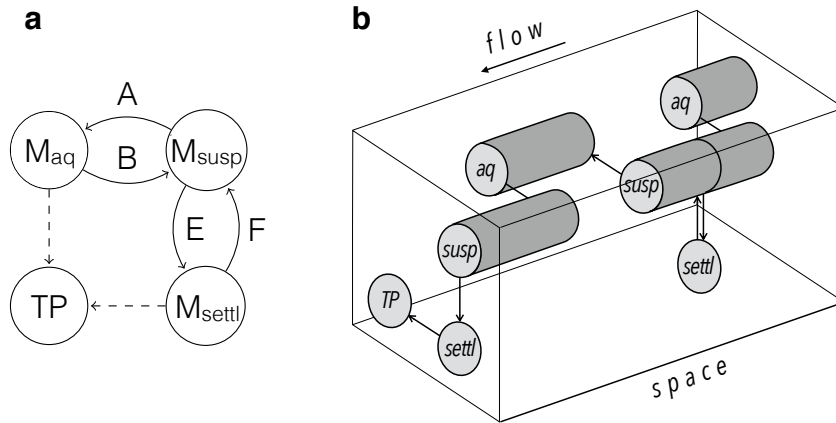
191 2.1 Partitioning and transformation in a stream reach

192 We focus on the parent compound (the API). It is assumed that the total mass of the
193 parent compound (M_{total}) is split between three different states: aqueous phase in water
194 column (M_{aq}), sorbed to a suspended particle in water column (M_{susp}), or in the settled
195 sediment (M_{settl}), including both aqueous state in porewater and being sorbed onto settled
196 particles. Processes connecting the different partitioned states are sorption, desorption,
197 settling, and resuspension (see Fig. 1 left).

198 We assume that sorbed fractions are not bioavailable, biotransformation from parent
199 compound to transformation products of any kind (TP) can happen only from the aqueous
200 phases in the water column and the sediment (e.g. from porewater) (see Fig. 1 a). This
201 does not contradict the fact that the majority of degrader biomass resides in biofilms cov-
202 ering resuspended or settled particles. It has been widely shown that the sorbed fraction is
203 hardly or not at all bioavailable to microorganisms (section 26.4 in [Schwarzenbach *et al.*,
204 2016]) and hence the degrader biomass must mainly feed on the aqueous phase, whose
205 renewal may be limited by the rate of desorption.

206 We furthermore assume a resuspension-settling equilibrium, which is reasonable for
 207 mean flow conditions. This means that both the settled active sediment layer and the sus-
 208 pended sediment stock are steady inside the reach. This obviously means that the model
 209 is invalid for conditions when this assumption is not met (e.g. under bed-moving floods or
 210 net deposition along the entire reach).

211 When all processes are first order with rate constants denoted by A to F (Fig. 1, A
 212 is the desorption rate constant, B is the sorption rate constant, E is the settling rate con-
 213 stant, and F is the resuspension rate constant), equilibrium partitioning can be expressed
 214 as $M_{aq}/M_{susp} = A/B$ and $M_{settl}/M_{susp} = E/F$ (see details in section S1 of the Support-
 215 ing Information [SI]). Furthermore, $M_{aq} + M_{susp} + M_{settl} = M_{total}$, so $M_{susp}/M_{total} =$
 216 $(A/B + 1 + E/F)^{-1}$. The dimensionless ratios A/B and E/F derive from the proper-
 217 ties of the stream reach and the API. A/B describes the sorption equilibrium between
 218 water and suspended sediment: $A/B = (K_d \cdot SSC)^{-1}$, where K_d is the sediment-water
 219 partitioning coefficient [$m^3 \text{ kg}^{-1}$], and SSC is the suspended sediment concentration [kg
 220 m^{-3}]. Similarly, E/F characterises the resuspension-settling equilibrium in the reach,
 221 $E/F = S(SSC \cdot Z_w)^{-1}$, where S is the resuspendable sediment stock in the active layer
 222 [kg m^{-2}], and Z_w is the water depth [m].



223 **Figure 1.** Partitioning and transformation pathways (a) and example for the flow-induced spiralling pattern
 224 in streams (b).

225 Transformation pathways are asymmetrical, they do not start from each state of the
 226 API and do not proceed at the same rates. They therefore slightly change the ratios be-
 227 tween different API states, but this remains negligible when transformation rate constants

228 are much smaller than $A - F$ (which is fulfilled for not readily degrading compounds, see
 229 section S1.1 in SI).

230 In a flowing system the partitioning cycle becomes a spiral, e.g. partitioning is su-
 231 perimposed with longitudinal displacement (just as a spiral stems from superimposing
 232 rotation and longitudinal movement). The spiral for a single molecule develops in a ran-
 233 dom way. Even in steady flow, displacement is not uniform as states M_{aq} and M_{susp} get
 234 carried downstream, but M_{settl} remains still (Fig. 1b). Propagation of the entire compound
 235 flux can be described by the mean of individual random spirals, where averaging smooths
 236 out randomness. The description of spiralling en masse requires expressing how parti-
 237 tioning affects mean downstream propagation (in terms of travel or residence time) and
 238 degradation kinetics at the system level. The first only depends on partitioning. The mean
 239 residence time of the parent compound in the control volume (τ^* [s]) relative to the mean
 240 water residence time (τ_w [s]), or retention, is simply:

$$241 \quad \frac{\tau^*}{\tau_w} = \frac{\frac{A}{B} + 1 + \frac{E}{F}}{1 + \frac{A}{B}} = 1 + \frac{\frac{S}{SSC \cdot Z_w}}{1 + \frac{1}{K_d \cdot SSC}} \quad (1)$$

242 For the derivation of this equation please see section S1.1 of the SI. The A/B ratio is
 243 actually the aqueous-sorbed ratio of the API in the water column, E/F is the settled-
 244 resuspended mass ratio of the sediment. The $\frac{\tau^*}{\tau_w}$ dimensionless factor corrects the water
 245 residence time for the fraction of the compound that is sorbed to the settled sediment and
 246 therefore cannot move with the flow of water and suspended particles.

247 The description of system-level degradation needs a concept that links the degrada-
 248 tion rate constants in the water and sediment compartments. The k'_{bio} concept introduced
 249 by *Honti et al.* [2016] does exactly this for compounds not subject to hydrolysis and pho-
 250 todegradation. The first order compartment-level biotransformation rate constant is the
 251 product of the second-order k'_{bio} constant, the particulate organic carbon concentration as
 252 a proxy for degrader biomass, and the aqueous (bioavailable) fraction of the compound in
 253 the specific compartment (Equations S15, S19 in the Supporting Information [SI]). Uti-
 254 lizing this connection between the first-order compartment-level rate constants, one can
 255 express their ratio using the dimensionless properties of the system (for details see section
 256 S2 in SI):

$$257 \quad \frac{k_{sed}}{k_w} = \frac{\frac{A}{B} + 1}{\frac{A}{B} \frac{F}{E} \frac{Z_a}{Z_w} + 1} = \frac{\frac{1}{K_d \cdot SSC} + 1}{\frac{Z_a}{K_d \cdot S} + 1} \quad (2)$$

258 where k_{sed} and k_w are first-order biotransformation rate constants [d^{-1}] in the sediment
 259 and in the water column, respectively. Z_a and Z_w are the depths of the active sediment
 260 layer and the water column [m], respectively.

261 The total-system biotransformation rate (k^* [d^{-1}]) is dependent on partitioning and
 262 the compartment-specific rates:

$$263 \quad k^* = \frac{M_{\text{aq}} + M_{\text{susp}}}{M_{\text{total}}} k_w + \frac{M_{\text{settl}}}{M_{\text{total}}} k_{\text{sed}} \quad (3)$$

264 This, relative to k_w becomes (for detailed derivation see section S2 in the SI):

$$265 \quad \frac{k^*}{k_w} = \frac{\frac{A}{B} + 1}{\frac{A}{B} + 1 + \frac{E}{F}} \left(1 + \frac{\frac{E}{F}}{\frac{A}{B} \frac{Z_a}{Z_w} + 1} \right) = \frac{\frac{1}{K_d \cdot \text{SSC}} + 1}{\frac{1}{K_d \cdot \text{SSC}} + 1 + \frac{S}{\text{SSC} \cdot Z_w}} \left(1 + \frac{\frac{S}{\text{SSC} \cdot Z_w}}{\frac{Z_a}{K_d \cdot S} + 1} \right) \quad (4)$$

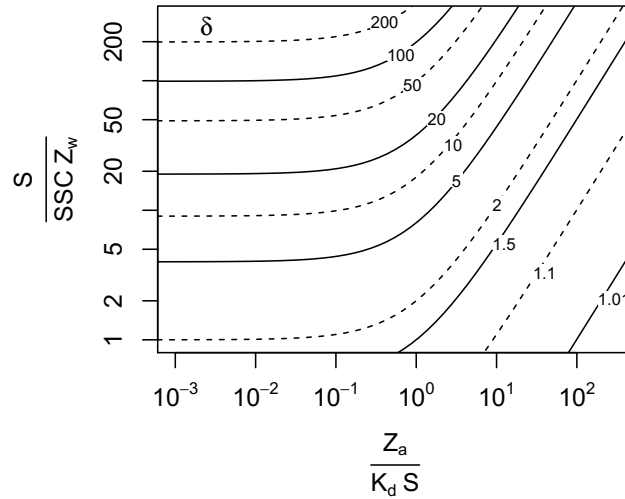
266 Multiplying equations (1) and (4) yields the sediment modification factor (δ [-]) for
 267 a single stream reach, which expresses the relative surplus biodegradation due to the pres-
 268 ence and activity of the settled sediment (through both retention and degradation):

$$269 \quad \delta = \frac{k^* \tau^*}{k_w \tau_w} = 1 + \frac{\frac{E}{F}}{\frac{A}{B} \frac{Z_a}{Z_w} + 1} = 1 + \frac{\frac{S}{\text{SSC} \cdot Z_w}}{\frac{Z_a}{K_d \cdot S} + 1} \quad (5)$$

270 where $\frac{S}{\text{SSC} \cdot Z_w}$ indicates the partitioning of the total sediment mass between the floating
 271 and settled phases, and $\frac{Z_a}{K_d \cdot S}$ is the aqueous-sorbed ratio inside the sediment. A detailed
 272 derivation of δ in terms of A/B , and E/F is presented in section S2 of the SI. If degra-
 273 dation pathways other than biotransformation (e.g., phototransformation or hydrolysis) are
 274 present, the equation determining δ needs some extension, but the model remains practi-
 275 cally the same (see section S3 in SI).

276 A value of $\delta = 2$ indicates that biotransformation of a compound in a river reach is
 277 twice what it would be in the absence of suspended and settled sediment. Stream proper-
 278 ties and sediment dynamics can easily raise δ far beyond 1 (Fig. 2) at almost any sorption
 279 behaviour. Interestingly, the water-sediment depth ratio (Z_w/Z_a) does not directly influence
 280 the dimensionless travel time (eq. (1)), but it plays a role in k^*/k_w and δ , especially for
 281 moderately hydrophobic compounds (Figure S3. in SI). The resuspension-settling equi-
 282 librium (E/F or $\frac{S}{\text{SSC} \cdot Z_w}$) seems to be the strongest factor affecting δ . Reaches of limited
 283 resuspension capacity (i.e., with large settled-resuspended ratio) degrade strongly sorbing
 284 compounds up to orders of magnitude faster than those having restricted sediment reten-
 285 tion ability (Fig. 2).

290 As δ accounts for degradation outside the water column, the output flux from the
 291 reach can be calculated by putting δ inside the equation describing a reach reactor without



286 **Figure 2.** The role of the sediment regime and sorption properties on the sediment modification factor (δ).
 287 $\frac{S}{SSC \cdot Z_w}$ is the ratio between the settled and resuspended sediment mass, $\frac{Z_a}{K_d \cdot S}$ is the aqueous-sorbed ratio of
 288 the API in the sediment. δ is the relative pace of biotransformation in a river reach relative to a sediment-less
 289 condition.

292 sediment:

$$293 \quad F_{\text{out}} = F_{\text{in}} \exp(-\delta k_w \tau_w) \quad (6)$$

294 where F_{in} , and F_{out} are the total incoming and outflowing fluxes of the parent compound
 295 for a single reach [kg d^{-1}], respectively.

296 2.2 Model of the stream network

297 The stream network was built up from river reaches. Local API removal was cal-
 298 culated in each reach according to the local value of k_w , δ , and τ_w . Since the model was
 299 first-order, the downstream effect of each pollution source could be computed indepen-
 300 dently and summed.

301 Inputs to the stream network are uncertain. While consumption patterns for the se-
 302 lected APIs can be assumed to vary little by region (within a single country), excretion
 303 rates and removal rates by wastewater treatment plants (WWTPs) are more uncertain.
 304 Therefore, to separate the uncertain proportion that never reaches the streams, the local
 305 input flux ($F_{\text{in,local}}$, [kg d^{-1}]) was written as the product of local consumption ($F_{\text{cons,local}}$,
 306 [kg d^{-1}]) and a unified escape rate ($k_{\text{esc}} = k_{\text{excr}}(1 - k_{\text{rem}})$ [-]), the product of the mean

human excretion rate (k_{excr}) and the proportion passing through the WWTP ($1 - k_{\text{rem}}$):

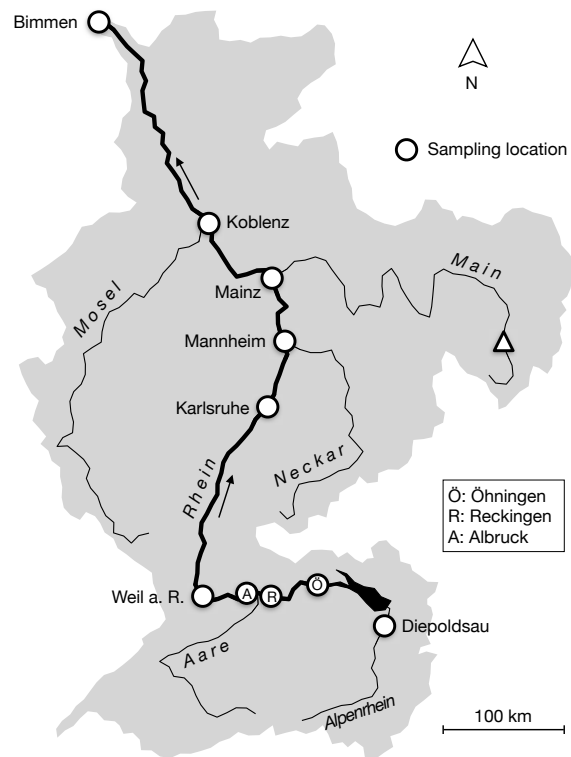
$$F_{\text{in,local}} = F_{\text{cons,local}} k_{\text{esc}} \quad (7)$$

Model inputs were:

1. A database of the 18240 reaches of the Rhine catchment upstream of the Dutch border (Bimmen) from the CCM2 river and catchment database (EU JRC, <http://ccm.jrc.ec.europa.eu/>, Fig. 3). Strahler stream order, drainage area [km^2], channel slope rounded to integer %, reach length, and ID of the downstream neighbour reach were given for each reach. Due to the very coarse resolution of channel slope data, slope values were averaged across neighbouring stream reaches weighted by drainage area (so that smaller steep streams cannot bias the mean slope of major rivers).
2. A table with consumption amounts for the selected APIs for each reach from the CrossWater project [Moser *et al.*, 2018].
3. A table with the observed weekly mean flux of the selected APIs for 16 sites from the Rhine and major incoming tributaries by Ruff *et al.* [2015] (Fig. 3).

A preprocessing step was carried out once to estimate mean physical properties for each reach based on drainage area and channel slope (see description in section S4 of the SI). Estimated channel geometry, flow velocity, sediment grain size distribution had to be used due to lack of measurements in sufficient density to cover the entire stream network. Mean suspended sediment concentrations (SSC) were derived from these parameters. In reality SSC is governed by discharge, season, the state of the upstream catchment and the stage of flood pulses, which together make it highly dynamic. We had to neglect this variability as we had no means to model dynamic SSC in the entire stream network. Products of the preprocessing step were first the water depth (Z_w), the mean flow velocity (U), the mean water residence time in the reach (τ_w), the settled sediment stock (S), SSC , the sediment mass median diameter (D_{50}), and finally E/F and Z_a/Z_w .

Calibrated model parameters were those where significant uncertainty was expected: K_d , k'_{bio} , and k_{esc} . K_d is weakly known for such a large and diverse system. It can be calculated as the product of $f_{\text{oc, sed}}$ (sediment organic carbon content [-]) and K_{oc} (the organic carbon-water partition coefficient, [$\text{L kg}_{\text{OC}}^{-1}$]), but reported K_{oc} values from regulatory and other studies show high variability. k'_{bio} was the primary target of our investigations. Values were extracted from OECD 308 studies for APIs wherever available, but



321 **Figure 3.** The Rhine catchment above the Dutch-German border, major rivers and sampling locations (open
 322 circles). The open triangle shows the upstream starting point of the profile in Figure 7.

340 they were at least as uncertain as K_d . k_{esc} encapsulates all API-related input-uncertainty,
341 including errors in consumption rates, excretion rates, and uncertainty and variability in
342 WWTP removal rates. The independent, normally distributed model error's standard devi-
343 ation was calibrated together with the model parameters.

344 In each model run, the model first calculated the values of A/B and δ for every
345 single reach. This was necessary because these quantities depend on K_d , which is cali-
346 brated. After this, travelling fluxes of APIs were calculated for each reach by assuming
347 both degradation and conservative behaviour. The likelihood of model parameters was cal-
348 culated at reaches where measurements were available.

349 The calibration procedure took place in a Bayesian framework. An informative prior
350 was assigned to k_{esc} : a lognormal distribution with the estimated mean values from *Singer*
351 *et al.* [2016] with a relative standard deviation of 15%, except for API13, where the pub-
352 lished value for k_{esc} was too low to justify the observations along the Rhine and therefore
353 a uniform distribution over the [0,1] domain was used ($k_{esc} = 0.25$ was necessary instead
354 of 0.09 to produce the observed flux without any degradation). The prior for K_{oc} was a
355 lognormal distribution with mean from OECD 106 experiments and 80% relative stan-
356 dard deviation. The prior for k'_{bio} was a uniform distribution over the technically feasible
357 numerical range (10^{-4} to 10^4 [L (d g OC) $^{-1}$]) to prevent mathematical instability. The pa-
358 rameter posterior was sampled by Markov chain Monte Carlo (MCMC) sampling.

359 **2.3 Model of OECD 308 experiments**

360 The model of *Honti et al.* [2016] was applied to obtain k'_{bio} from 10 OECD 308 ex-
361 periments featuring the 4 compounds API6, API8, API9, and API13. Data were extracted
362 from confidential dossiers provided by the German Environment Agency [*Fenner et al.*,
363 2016]. Concentration time-series were derived from duplicate measurements by averaging.
364 Experimental meta-data belonging to or required for interpretation of OECD 308 were
365 extracted from the dossiers as well, such as results of OECD 106 sorption experiments.
366 Calibration again took place in a Bayesian framework, the same priors were used for K_{oc}
367 and k'_{bio} as in the calibration of the stream network model.

3 Results

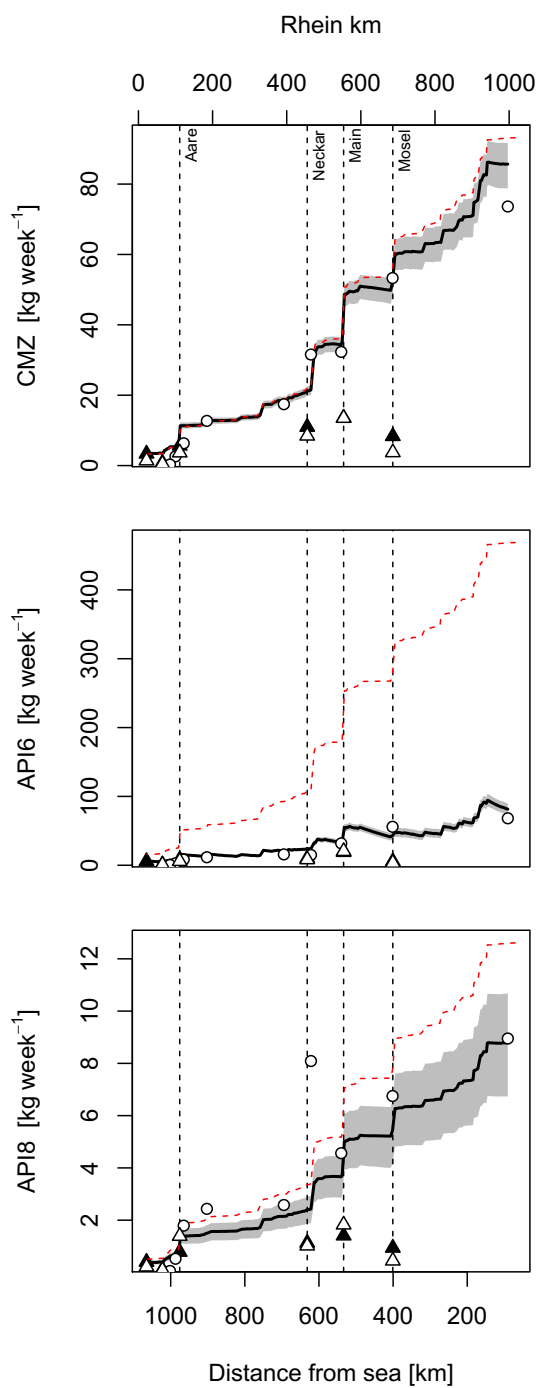
3.1 Degradation of APIs in the Rhine basin

Simulated longitudinal profiles of API fluxes were in good agreement with the measurements for all APIs (Fig. 4, section S6 in SI). Given that *Ruff et al.* [2015] report about 20% measurement accuracy, calibration fulfilled expectations. The only significant discrepancy between measured and modelled values was the model's inability to fit to a probably erroneous measured point for API8. Less severe, yet systematic deviations were observed at the last measurement point (Bimmen). Here, the model was overestimating the local flux for all compounds except API8 by 5 to 25%. Possible explanations for this systematic error are (i) errors in the physical calculations for the lowermost sections of the Rhine affecting flow velocities or SSCs, (ii) regional deviations in the load/emission data, or (iii) incomplete mixing of shoreline plumes or cross-sectionally not representative sampling.

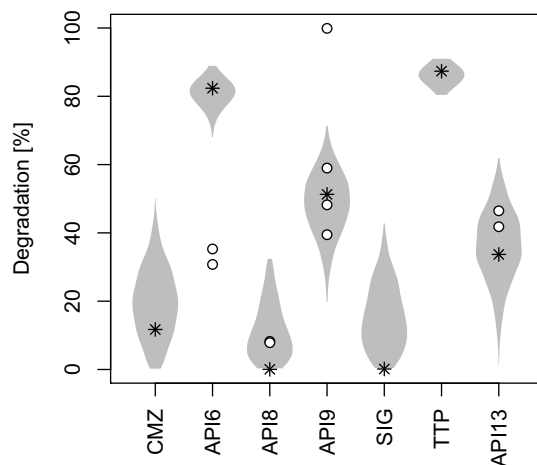
Out of the 7 APIs, two showed fast and efficient degradation in the stream network (API6, TTP), one was moderately degrading (API9), and three were practically conservative (CMZ, API8, SIG; Fig. 5). Due to the uncertainty of k_{esc} , the modelled degradation of API13 varied between limited and moderate. Based on previous experience, CMZ was expected to be conservative, which was not contradicted by the model results (but API8 and SIG were even "more conservative", showing even less degradation).

There was a clear relationship between simulated degradation in the stream network and the calibrated Rhine k'_{bio} values, which was no surprise considering the model mechanisms. Differences in sorption properties of the individual compounds did not strongly influence the correspondence between k'_{bio} and degradation. Below the k'_{bio} value of 40 [L (d g OC)⁻¹] compounds were not degraded noticeably. Values above 200 led to 80-90% degradation.

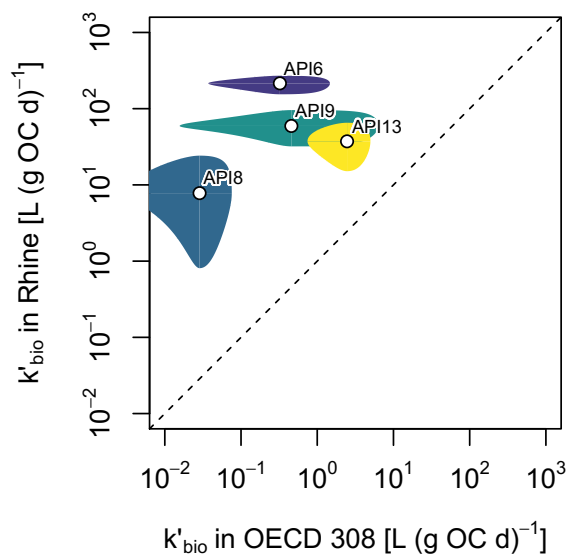
One noteworthy aspect is that measured longitudinal flux profiles of both conservative and degrading compounds look very similar, i.e., there is a pattern of increasing load downstream (Figs. 4, 7). This behavior was well mirrored by the modelled profiles. The reason why degradation did not leave a recognizable imprint on the shape of the profile in the Rhine river is that – according to the model – none of the compounds degraded significantly in higher order streams (over Strahler orders 5-6), especially not in the Rhine itself



381 **Figure 4.** Modelled and measured flux profiles of selected APIs along the Rhine. Open symbols: mea-
 382 surements (circles: Rhine, triangles: tributaries), closed triangles: modelled values for tributary inflows.
 383 Climbing dashed line: conservative assumption (accumulated load). Black line: best model fit. Grey band:
 384 95% uncertainty interval. Note: open triangles may hide closed ones on perfect coincidence.



391 **Figure 5.** Modelled total degradation of APIs in the Rhine basin (violins, with asterisk indicating the
 392 maximum likelihood values) and in OECD 308 experiments (open dots, values at 14 days after experiment
 393 start).



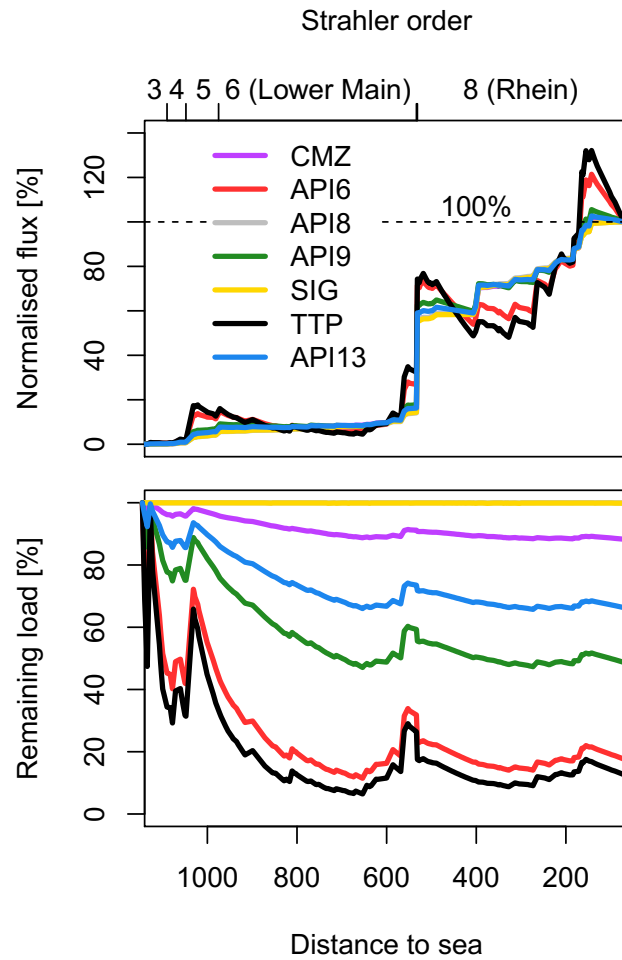
400 **Figure 6.** Relationship between k'_{bio} in the Rhine basin and k'_{bio} derived from OECD 308 and field data.
 401 The dashed line indicates the 1:1 line.

408 (Fig. 7). The model suggests that if there was any degradation, it rather happened in the
409 small and medium-sized streams (up to Strahler order 4). In the higher order streams the
410 high Z_w/Z_a ratio and low SSC (see Fig. S5 in SI) prevented significant biotransformation.
411 In addition to this physical dependence on stream size, the majority of emission sources
412 concentrate around lower order reaches (Fig. 8 top). Due to the lack of degradation in the
413 Rhine, the incoming tributary loads are largely preserved until the outflow, regardless of
414 the compound's degradability, and hence accumulate along the Rhine. As a result, loads
415 of wastewater-related contaminants in the Rhine roughly scale with catchment area and
416 hence steadily grow along the river.

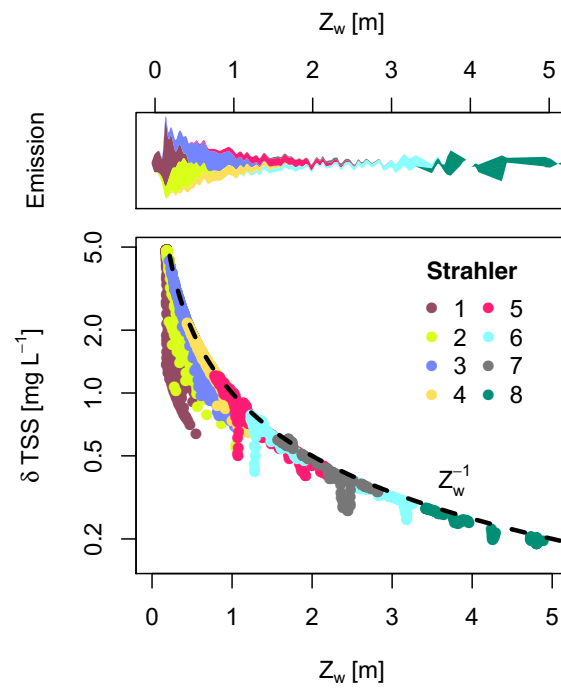
421 Based on the calculated A/B , E/F , and Z_a/Z_w values of the stream reaches, δ was
422 typically in the range of 4–13 (90% range). This indicates that the total system degra-
423 dation was everywhere much faster than degradation in water alone. This is in line with
424 the experience gained in laboratory water-sediment systems, such as OECD 308 and 309
425 [Honti and Fenner, 2015; Honti et al., 2016; Shrestha et al., 2016]. However, due to the
426 usually very low rate of degradation in water, such high multiplier values still could not
427 guarantee that the overall degradation was observable in all parts of the stream network.
428 The pace of degradation relative to k'_{bio} ($\frac{k^*}{k'_{\text{bio}}} \approx \delta \text{SSC}$) followed a rather simple pattern
429 everywhere. It was proportional to the inverse of water depth (Z_w^{-1} , Fig. 8). Such a close
430 relationship between Z_w^{-1} and δSSC is probably case-specific and was caused by the lack
431 of physical data from the stream network. As all reach parameters were inferred from the
432 two numbers for drainage area and slope, we must have underestimated the physical vari-
433 ability among similarly-sized reaches and consequently the variability in their degradation
434 capacity.

438 3.2 Comparison to degradation in OECD 308 systems

439 The k'_{bio} values from OECD 308 experiments were lower than the values deduced
440 from field data for all 4 compounds having both types of data (Fig. 6). The difference can
441 presumably be attributed to the fact that APIs were exposed to more diverse degraders and
442 degradation pathways during their travel in the Rhine basin than during being trapped in
443 the closed experimental vessels (i.e., deeper oxic layers due to turbulence, more exchange
444 between settled and suspended phase, more diverse microbial communities, etc.). To more
445 directly evaluate the outcome of OECD 308 experiments against field observations, we
446 also sought to directly compare degradation between the two systems. We found that



417 **Figure 7.** Modelled downstream profile through River Rednitz, River Main and the Rhine starting from
 418 near Ansbach. Top: flux of APIs normalised by the value at Bimmen, bottom: proportion of the total up-
 419 stream load remaining in the river. The jump from Strahler order 6 to 8 is the confluence with the Rhine at
 420 Mainz, the jump from 4 to 5 is the confluence with the Main at Bamberg.



435 **Figure 8.** The role of water depth (Z_w) in the modelled relative degradation rate constants (δ SSC). Col-
 436 ors indicate the Strahler stream order of reaches, the upper panel shows a streamplot of emissions into the
 437 differently sized and ordered reaches (the local height of patches is proportional to the emission in [g d^{-1}]).

447 degradation in the Rhine catchment (upstream of Bimmen) and during approximately the
448 first 14 days of the OECD 308 experiments generally showed qualitative agreement (Fig-
449 ure 5). The 14 days period was selected because it was comparable to the mean residence
450 time in the Rhine Basin (free flowing time: 7 days) and being reported in the OECD 308
451 dossiers of all 4 compounds. The only exception from the qualitative agreement was API6
452 that showed only about half the degradation in the OECD 308 experiment compared to
453 its degradation in the Rhine, suggesting additional degradation mechanisms that are not
454 present in simulation tests but are relevant in the field, e.g., direct or indirect photolysis.
455 This is also reflected by the fact that API6 shows the highest discrepancy between field
456 and experimental k'_{bio} amongst the four compounds for which this comparison was pos-
457 sible. It needs to be kept in mind though that the above comparisons are not very robust
458 due to the problems of identifying k'_{bio} from field data (see below) and the high variabil-
459 ity of k'_{bio} values derived from OECD 308 data. The latter is nicely illustrated by API9:
460 degradation in OECD 308 by day 14 varied between 59% and 99% for two experiments
461 carried out with the very same sediment.

462 **3.3 Importance of input uncertainty**

463 The increasing longitudinal flux profiles cause a practical problem. As the smaller
464 streams where the majority of degradation takes place are much shorter than the large
465 rivers, the corresponding flux profiles taken from the Rhine (or main rivers) all resem-
466 ble the profile of a conservative compound. Therefore, when the actual emission rates of
467 a certain API from WWTPs are not or only weakly known, uncertainty heavily influences
468 the inferred degradation rates, causing a strong positive correlation between k_{esc} and k'_{bio}
469 (section S5 in SI). This is possible because the degrading and non-degrading profiles show
470 only small differences (Fig. 7 top) that can easily remain unnoticed when measurement
471 points are sparsely distributed and flux estimations have an admitted accuracy of about
472 20%.

4 Discussion

4.1 Biodegradation in the Rhine and in the laboratory

The systematically larger k'_{bio} values from the Rhine basin compared to OECD 308 experiments could be logically interpreted as the result of reduced microbial diversity and the ensuing lack of certain transformation pathways in the experimental systems.

The comparison of field-laboratory rates for abiotic processes often come up with the opposite conclusion: well-mixed laboratory systems show higher complexing, weathering, and dissolution rate constants than real catchments [Pačes, 1983; Swoboda-Colberg and Drever, 1993; Liu *et al.*, 2013; Wen and Li, 2018] due to hindrances of mass transfer and higher spatial heterogeneity in streams. The case of biotransformation and OECD 308 is somewhat different. From the physical side, contrary to the abiotic systems cited above, the stagnant OECD 308 is obviously less well mixed than any stream, so the mass transfer would be more effective in the field, facilitating a faster degradation. From the chemical side, the sediment of OECD 308 is anaerobic except for a very thin surface layer, which decreases the number of potential transformation pathways for most APIs, while stream sediments are typically aerobic in the first few cm. OECD 308 must be performed in darkness, which excludes the possibility of phototransformation, while streams are at least partially exposed to sunlight. From the biological side, microbial diversity is a key factor in biotransformation of organic micropollutants and therefore higher physical and chemical heterogeneity – which are evidences for ineffective mass transfer, yet support higher microbial diversity – should basically increase the number of transformation pathways. The pre-incubation of the OECD 308 system before spiking the API is likely to exert a strong selective pressure on the microbiota, lowering diversity and thereby the number of effective heterotrophic transformation pathways. These factors altogether mean that OECD 308 suffers from both mass transfer limitation and a relative scarcity of transformation pathways, which explains observing lower first-order degradation rate constants and longer half-lives.

However, it has to be noted that both sets of calibrated biotransformation rate constants are conditional on the structures of the corresponding mathematical models. Potential structural deficiencies – like a missing mechanism, e.g. phototransformation – and wrong parameterizations – like biased expectations on certain parameters – can also produce systematic deviations between the two sets. As no model is surely free from such

505 defects, it cannot be proven whether the apparently higher degradation rate constants of
506 the Rhine indeed reflect the effect of the better mixed yet still more diverse stream envi-
507 ronment.

508 Nevertheless, we have found qualitative agreement between degradation in the first
509 14 days of OECD 308 and degradation in the Rhine Basin upstream of Bimmen (Fig. 5),
510 but the small number of involved compounds did not allow us to judge the strength of this
511 agreement statistically. While extending the analysis to more compounds could fix the sta-
512 tistical issue and prove or refute this specific agreement, other subcatchments in the Rhine
513 Basin or other river basins would certainly show different relationships. Other catchments
514 with different catchment size, distribution of stream orders, reach length, residence time
515 and sediment conditions would potentially remove different amounts of APIs. However,
516 the model suggests that there is a reduction in differences between sufficiently large river
517 basins in terms of API removal. As biotransformation concentrates in small and medium-
518 sized streams, one can expect that total removal does not increase linearly with stream
519 length and basin size. Our model showed that after 1-2 days of mean water residence time
520 (approximately 2-4 days free flowing time from the most distant source to the subcatch-
521 ment outlet) subcatchment-specific removal rates stabilise. This coincides with the onset
522 of stream orders 6-7. Therefore, if other conditions were similar, basins with a main river
523 over Strahler order 6 should have more similar removal rates than smaller ones. Therefore,
524 if a simulation test represents degradation in a large river basin, from a physical point of
525 view it is likely to represent other large basins as well.

526 **4.2 Representativeness of simulation tests**

527 In the limited spectrum of physical properties represented by the modelled reaches
528 of the Rhine, stream network degradation could vary between extremely slow (in the ma-
529 jor channels) and rather fast (headwaters) for the same compound. Such high variability of
530 the actual in-stream degradation highlights that it is illusory to think that experimentally
531 derived half-lives represent at least a considerable proportion of the environment. Accord-
532 ing to our model, half-lives can vary over orders of magnitude in the stream network due
533 to the different physical properties of stream reaches (Figs. 2, S3), while we did not even
534 consider changes in microbial community composition along the stream network. Simu-
535 lation tests such as OECD 308 and 309 define very specific conditions and therefore are
536 able to simulate the compound's behaviour in tiny niches of the environmental spectrum.

537 Thus, instead of the current risk assessment practice of projecting experimental
538 half-lives to the environment in general, it would be preferable to view simulation tests
539 as more (OECD 308) or less (varieties of OECD 309) standardised ways of deducing
540 environment-invariant properties of the compound (such as k'_{bio} , or A/B) that can after-
541 wards be used to estimate half-lives under different environmental conditions.

542 In this respect, however, both OECD 308 and 309 suffer from serious drawbacks.
543 Beyond their considerable costs and effort requirements, they fail to provide relevant in-
544 formation for persistence modelling in most kinds of streams. The presented model can
545 be used to demonstrate this, but findings are not conditional on the model assumptions.
546 In the current model, A/B and E/F are the most important physical (partitioning) factors
547 modulating the rate of degradation. Even when carried out with the sediment in question,
548 OECD 308 does not provide useful information on any of them: there is hardly any sus-
549 pended sediment in the water column of OECD 308 experiments, so sorption to suspended
550 solids (from which A/B could be derived) or partitioning between suspended and settled
551 phases (E/F) cannot be measured. Instead, sorption influences the compound's distribution
552 inside the sediment and, as a consequence, diffusion between the water and sediment lay-
553 ers, yet these processes are difficult to extract from the measured concentration patterns.
554 Accordingly, while k'_{bio} can be derived from OECD 308, it is quite uncertain due to the
555 interaction between these processes [Honti *et al.*, 2016]. While it is not surprising that
556 the stagnant OECD 308 experiments does not represent streams too well, the problems of
557 OECD 309 experiments in doing so are more surprising. In the non-pelagic versions of
558 OECD 309, there is sorption to suspended sediment and hence A/B and its effect on k'_{bio}
559 should theoretically be observable. However, since SSCs in such systems are quite low,
560 biodegradation is rather limited in practice. As a consequence, while information can be
561 gained on A/B there is little information to be learned on k'_{bio} from these experiments.
562 Thus, OECD 309 experiments tend to be very expensive hydrolysis experiments rather
563 than actual biodegradation tests. Moreover, because the sediment is kept in suspension in
564 these experiments, there is no way to learn anything about the influence of settling (i.e.,
565 E/F) on degradation.

566 From a modelling perspective, a hybrid (flume or stirred) experiment with both sus-
567 pended particles and settled sediment could be a better solution. By carrying out such
568 experiments with different settings (different SSC – but enough to stimulate observable

569 degradation, S) one could determine all critical model parameters with reasonable accu-
570 racy.

571 **4.3 Behaviour of stream networks and input uncertainty**

572 According to our model, whenever degradation happened, it was in the small and
573 medium tributaries. Large streams acted as conveyor belts forwarding all incoming pollu-
574 tion towards the North Sea. *Boeije* [2000] found the same with GREAT-ER on a different
575 basis: they attributed degradation in the sediment entirely to surface biofilms (which may
576 not be a proper assumption in larger, deep streams) and concluded that increasing stream
577 size reduces exposure to sediment and therefore elongates half-lives. Half-lives in small
578 creeks can be 60 times shorter than in large rivers [*Boeije*, 2000]. The cross-sectional
579 area-volume ratios identified as primary physical determinants of degradation half-lives
580 by *Boeije* [2000] are equivalent to the hydraulic radius, which is approximately equal to
581 Z_w in natural channels (compare Fig. 8). The negative scaling of biodegradation potential
582 with stream size is not limited to micropollutants. *Alexander et al.* [2000] found similar
583 patterns for nitrogen.

584 Considering the suggested place of degradation (small-medium streams), the posi-
585 tions of measurement locations were suboptimal. As all points were along the Rhine, in
586 either the Rhine itself or in the mouths of major tributaries, measured fluxes bore no in-
587 formation about what happened in the upstream focal regions of degradation. One could
588 argue that measurement locations should have been positioned in smaller streams as well,
589 but there is the aspect of size too. The upstream catchment above a measurement loca-
590 tion must be large enough to smooth out temporal and spatial variability of pollution
591 sources and must host enough inhabitants to produce a clear chemical signal. Therefore,
592 the placement of measurement locations needs a careful balancing. Starting and endpoints
593 of longer sections of medium-sized tributaries without significant lateral inputs could be
594 optimal points for future sampling campaigns.

595 As we found no way to infer degradation from the observed fluxes alone, the model's
596 findings about degradation are conditional on the input data: the national consumption
597 statistics, and the estimated consumer excretion and WWTP removal rates taken from
598 *Singer et al.* [2016].

599 For conservative APIs we found that the emissions calculated from consumption
600 data from *Moser et al.* [2018], and the consumer excretion rates plus WWTP removal rates
601 from *Singer et al.* [2016] nicely matched the observed flux data of [*Ruff et al.*, 2015] for
602 almost each measurement point. This fact makes the same likely for the degrading com-
603 pounds, thereby indirectly supporting our statements on the extent and place of degrada-
604 tion.

605 The difficulty of separating emissions from degradation has already been described
606 by *Pistocchi et al.* [2012] in the context of a totally different model framework. They also
607 concluded that emission–half-life combinations can be identified, but none of them sepa-
608 rately. Knowledge of either is necessary to estimate the other from field data.

609 For large river systems pollutants will make the majority of their travel (distance-
610 wise) inevitably in large streams. Due to the accumulating nature of large rivers this means
611 that sampling along the main channels will reflect a picture that is very similar to the be-
612 haviour of a conservative compound. This suggests that for compounds without a solid
613 consumption and emission data foundation the estimation of degradation parameters can
614 become impossible.

615 **4.4 Sediment behaviour**

616 Sediment dynamics is a cornerstone of our model, as it influences δ via E/F . Ac-
617 cording to the SSC estimation method described in section S4, the streams of the Rhine
618 basin seem to be generally sediment-poor. Suspended loads are far below the hydraulic
619 carrying capacity of flow (see section S4 in SI). Internal sediment supply is the only pos-
620 sible major supplier of SSC during low and medium flow when surface runoff is negligi-
621 ble. Compared to common definitions of the “active” sediment layer from a sedimentol-
622 ogy perspective (about 3 times the 90th percentile grainsize diameter [D_{90}] or the median
623 grainsize diameter [D_{50}]), even such low SSCs require intensive exchange between the
624 water column and the active layer. In that case, however, the common concept of the sedi-
625 ment as a relatively stable sink for pollutants is wrong. A simple calculation can estimate
626 the order of magnitude of residence times in the active layer. An average sand particle
627 with $D=0.5$ mm has a terminal settling velocity around 5-10 cm/s. Considering an SSC of
628 30 [mg L^{-1}], and $Z = 5$ [m] (all values are typical for the Rhine) the downward settling
629 flux is about 0.002 [$\text{kg m}^{-2} \text{s}^{-1}$], which – in equilibrium – must be paired by a similar

630 upward flux. Even with an active layer depth of $Z_a = 3$ [cm] (upper limit of calculated
631 values for stream reaches of Strahler orders 6–8), and porosity of 50%, the average par-
632 ticle residence time in the active layer is as little as 5 hours in steady low and medium
633 flow. Unsteady flow and especially bed-moving floods are expected to further shorten this
634 period. Thus, unless a protective biofilm develops altering particle exchange between the
635 water column and the sediment [Vignaga *et al.*, 2013], in larger streams the active layer is
636 likely to be restructured at subdaily frequency, which is in strong contrast with a typical
637 lake sediment and the experimental conditions in OECD 308.

638 5 Conclusions

- 639 • The persistence of active pharmaceutical ingredients could not be evaluated from
640 concentration patterns in the field alone. Rather, precise emission rates (consump-
641 tion, consumer excretion, removal in WWTPs) need to be known together with an
642 approximate K_d . Otherwise emissions, sorption, and degradation can compensate
643 for each other's effect, which renders the identification of actual degradation impos-
644 sible.
- 645 • Persistence suggested by simulation tests did not robustly match persistence inferred
646 from field observations. According to the model calibration, k'_{bio} is higher in rivers
647 than in OECD 308, probably due to the higher variety of processes that facilitate
648 biotransformation. Candidates for such processes are turbulence and mixing, tem-
649 perature, light exposure, and higher diversity of degrader microfauna.
- 650 • Despite the higher calibrated values of k'_{bio} , the Rhine stream network cannot de-
651 grade higher proportions of emitted APIs than the first 14 days of an OECD 308
652 experiment. This is explained by the (i) lack of time, and (ii) limited exposure to
653 degrader biomass in the main rivers.
- 654 • Our model suggests that physical conditions seriously limit exposure to degrader
655 biomass above Strahler stream orders 5–6. Therefore streams of order 1–5 can be
656 considered as hotspots for biodegradation in the Rhine Basin.

657 Acknowledgments

658 The PIdent project was supported and the OECD 308 data were provided by the German
659 Environment Agency (Umweltbundesamt) under contract FKZ 3715 65 415 3. Emission
660 data from the CrossWater project financed by the Swiss National Science Foundation

661 (Grant no. 406140-125866) is gratefully acknowledged. We thank Daniela Gildemeister
662 and Janina Wöltjen from the German Environment Agency for their constructive com-
663 ments on the manuscript. Data used in this study are available in public repositories, ex-
664 cept the confidential results of the OECD 308 experiments, which are managed by the
665 German Environment Agency (Umweltbundesamt). GIS data on subcatchments, river seg-
666 ments and topology, people equivalents are available at doi:10.5281/zenodo.556143, API
667 consumption and removal in wastewater treatment plants at doi:10.1021/acs.est.5b03332,
668 monitored data in the Rhine at doi:10.1016/j.watres.2015.09.017.

669 **References**

- 670 Alexander, R. B., R. A. Smith, and G. E. Schwarz (2000), Effect of stream channel size
671 on the delivery of nitrogen to the Gulf of Mexico, *Nature*, 403(6771), 758–761, doi:
672 10.1038/35001562.
- 673 Boeije, G. (2000), Incorporation of biofilm activity in river biodegradation modeling: a
674 case study for linear alkylbenzene sulphonate (LAS), *Water Research*, 34(5), 1479–
675 1486, doi:10.1016/s0043-1354(99)00279-1.
- 676 Boethling, R., K. Fenner, P. Howard, G. Klečka, T. Madsen, J. R. Snape, and M. J. Whe-
677 lan (2009), Environmental persistence of organic pollutants: Guidance for development
678 and review of POP risk profiles, *Integrated Environmental Assessment and Management*,
679 5(4), 539, doi:10.1897/ieam_2008-090.1.
- 680 Davis, J., S. Gonsior, G. Marty, and J. Ariano (2005), The transformation of hexabromo-
681 cyclododecane in aerobic and anaerobic soils and aquatic sediments, *Water Research*,
682 39(6), 1075–1084, doi:10.1016/j.watres.2004.11.024.
- 683 Ensign, S. H., and M. W. Doyle (2006), Nutrient spiraling in streams and river networks,
684 *Journal of Geophysical Research: Biogeosciences*, 111(G4), doi:10.1029/2005jg000114.
- 685 Ericson, J. F. (2007), An evaluation of the OECD 308 water/sediment systems for inves-
686 tigating the biodegradation of pharmaceuticals, *Environmental Science & Technology*,
687 41(16), 5803–5811, doi:10.1021/es063043+, pMID: 17874790.
- 688 Ericson, J. F., R. M. Smith, G. Roberts, B. Hannah, B. Hoeger, and J. Ryan (2013),
689 Experiences with the OECD 308 transformation test: A human pharmaceutical per-
690 spective, *Integrated Environmental Assessment and Management*, 10(1), 114–124, doi:
691 10.1002/ieam.1457.

692 Feijtel, T., G. Boeije, M. Matthies, A. Young, G. Morris, C. Gandolfi, B. Hansen,
693 K. Fox, M. Holt, V. Koch, R. Schroder, G. Cassani, D. Schowanek, J. Rosenblom, and
694 H. Niessen (1997), Development of a geography-referenced regional exposure assess-
695 ment tool for European rivers - GREAT-ER contribution to GREAT-ER #1, *Chemo-*
696 *sphere*, 34(11), 2351–2373, doi:10.1016/s0045-6535(97)00048-9.

697 Fenner, K., M. Honti, C. Stamm, L. Varga, and F. Bischoff (2016), Suitability of labora-
698 tory simulation tests for the identification of persistence in surface waters, *Tech. Rep.*
699 *FKZ 3715 65 415 3*, German Environment Agency (Umweltbundesamt), Dessau, Ger-
700 many.

701 Fono, L. J., E. P. Kolodziej, and D. L. Sedlak (2006), Attenuation of wastewater-derived
702 contaminants in an effluent-dominated river, *Environmental Science & Technology*,
703 40(23), 7257–7262, doi:10.1021/es061308e.

704 Honti, M., and K. Fenner (2015), Deriving persistence indicators from regulatory water-
705 sediment studies – opportunities and limitations in OECD 308 data, *Environmental Sci-*
706 *ence & Technology*, 49(10), 5879–5886, doi:10.1021/acs.est.5b00788.

707 Honti, M., S. Hahn, D. Hennecke, T. Junker, P. Shrestha, and K. Fenner (2016), Bridging
708 across OECD 308 and 309 data in search of a robust biotransformation indicator, *Envi-*
709 *ronmental Science & Technology*, 50(13), 6865–6872, doi:10.1021/acs.est.6b01097.

710 Huntscha, S., H. Singer, S. Canonica, R. P. Schwarzenbach, and K. Fenner (2008), Input
711 dynamics and fate in surface water of the herbicide metolachlor and of its highly mobile
712 transformation product metolachlor ESA, *Environmental Science & Technology*, 42(15),
713 5507–5513, doi:10.1021/es800395c.

714 Ingold, K., A. Moser, F. Metz, L. Herzog, H.-P. Bader, R. Scheidegger, and C. Stamm
715 (2018), Misfit between physical affectedness and regulatory embeddedness: The case of
716 drinking water supply along the Rhine River, *Global Environmental Change*, 48, 136–
717 150, doi:10.1016/j.gloenvcha.2017.11.006.

718 Koormann, F., J. Rominger, D. Schowanek, J.-O. Wagner, R. Schröder, T. Wind, M. Sil-
719 vani, and M. Whelan (2006), Modeling the fate of down-the-drain chemicals in rivers:
720 An improved software for GREAT-ER, *Environmental Modelling & Software*, 21(7),
721 925–936, doi:10.1016/j.envsoft.2005.04.009.

722 Kunkel, U., and M. Radke (2008), Biodegradation of acidic pharmaceuticals in bed sed-
723 iments: Insight from a laboratory experiment, *Environmental Science & Technology*,
724 42(19), 7273–7279, doi:10.1021/es801562j.

- 725 Li, Z., A. Sobek, and M. Radke (2015), Flume experiments to investigate the environmen-
726 tal fate of pharmaceuticals and their transformation products in streams, *Environmental*
727 *Science & Technology*, 49(10), 6009–6017, doi:10.1021/acs.est.5b00273.
- 728 Liber, K., K. R. Solomon, and J. H. Carey (1997), Persistence and fate of 2,3,4,6-
729 tetrachlorophenol and pentachlorophenol in limnocorrals, *Environmental Toxicology and*
730 *Chemistry*, 16(2), 293–305, doi:10.1002/etc.5620160227.
- 731 Lindim, C., J. van Gils, and I. Cousins (2016), A large-scale model for simulating the fate
732 & transport of organic contaminants in river basins, *Chemosphere*, 144, 803–810, doi:
733 10.1016/j.chemosphere.2015.09.051.
- 734 Liu, C., J. Shang, S. Kerisit, J. M. Zachara, and W. Zhu (2013), Scale-dependent rates of
735 uranyl surface complexation reaction in sediments, *Geochimica et Cosmochimica Acta*,
736 105, 326–341, doi:10.1016/j.gca.2012.12.003.
- 737 Moser, A., D. Wemyss, R. Scheidegger, F. Fenicia, M. Honti, and C. Stamm (2018), Mod-
738 elling biocide and herbicide concentrations in catchments of the Rhine basin, *Hydrology*
739 *and Earth System Sciences*, 22(8), 4229–4249, doi:10.5194/hess-22-4229-201.
- 740 Newbold, J. D., J. W. Elwood, R. V. O’Neill, and W. V. Winkle (1981), Measuring nu-
741 trient spiralling in streams, *Canadian Journal of Fisheries and Aquatic Sciences*, 38(7),
742 860–863, doi:10.1139/f81-114.
- 743 Pačes, T. (1983), Rate constants of dissolution derived from the measurements of mass
744 balance in hydrological catchments, *Geochimica et Cosmochimica Acta*, 47(11), 1855–
745 1863, doi:10.1016/0016-7037(83)90202-8.
- 746 Pistocchi, A., D. Marinov, S. Pontes, and B. M. Gawlik (2012), Continental scale inverse
747 modeling of common organic water contaminants in European rivers, *Environmental*
748 *Pollution*, 162, 159–167, doi:10.1016/j.envpol.2011.10.031.
- 749 Radke, M., and M. P. Maier (2014), Lessons learned from water/sediment-testing of phar-
750 maceuticals, *Water Research*, 55, 63–73, doi:10.1016/j.watres.2014.02.012.
- 751 Ruff, M., M. S. Mueller, M. Loos, and H. P. Singer (2015), Quantitative target and sys-
752 tematic non-target analysis of polar organic micro-pollutants along the river Rhine using
753 high-resolution mass-spectrometry – identification of unknown sources and compounds,
754 *Water Research*, 87, 145–154, doi:10.1016/j.watres.2015.09.017.
- 755 Schwarzenbach, R. P., P. M. Gschwend, and D. M. Imboden (2016), *Environmental Or-*
756 *ganic Chemistry, 3rd Edition*, NJ USA, John Wiley, ISBN: 978-1-118-76723-8.

757 Shrestha, P., T. Junker, K. Fenner, S. Hahn, M. Honti, R. Bakkour, C. Diaz, and D. Hen-
758 necke (2016), Simulation studies to explore biodegradation in water–sediment systems:
759 From OECD 308 to OECD 309, *Environmental Science & Technology*, 50(13), 6856–
760 6864, doi:10.1021/acs.est.6b01095.

761 Singer, H. P., A. E. Wössner, C. S. McArdell, and K. Fenner (2016), Rapid screening
762 for exposure to “non-target” pharmaceuticals from wastewater effluents by combining
763 HRMS-based suspect screening and exposure modeling, *Environmental Science & Tech-*
764 *nology*, 50(13), 6698–6707, doi:10.1021/acs.est.5b03332.

765 Solomon, K. R., J. Y. Yoo, D. Lean, N. K. Kaushik, K. E. Day, and G. L. Stephenson
766 (1985), Dissipation of permethrin in limnocorrals, *Canadian Journal of Fisheries and*
767 *Aquatic Sciences*, 42(1), 70–76, doi:10.1139/f85-009.

768 Swoboda-Colberg, N. G., and J. I. Drever (1993), Mineral dissolution rates in plot-
769 scale field and laboratory experiments, *Chemical Geology*, 105(1-3), 51–69, doi:
770 10.1016/0009-2541(93)90118-3.

771 Tixier, C., H. P. Singer, S. Canonica, and S. R. Müller (2002), Phototransformation of tri-
772 closan in surface waters: a relevant elimination process for this widely used Biocide-
773 Laboratory studies, field measurements, and modeling, *Environmental Science & Tech-*
774 *nology*, 36(16), 3482–3489, doi:10.1021/es025647t.

775 Tixier, C., H. P. Singer, S. Oellers, and S. R. Müller (2003), Occurrence and fate of car-
776 bamazepine, clofibric acid, diclofenac, ibuprofen, ketoprofen, and naproxen in surface
777 waters, *Environmental Science & Technology*, 37(6), 1061–1068, doi:10.1021/es025834r.

778 Trapp, S., and M. Matthies (1998), *Chemodynamics and Environmental Modeling*, Springer
779 Berlin Heidelberg, doi:10.1007/978-3-642-80429-8.

780 Vignaga, E., D. M. Sloan, X. Luo, H. Haynes, V. R. Phoenix, and W. T. Sloan (2013),
781 Erosion of biofilm-bound fluvial sediments, *Nature Geoscience*, 6(9), 770–774, doi:
782 10.1038/ngeo1891.

783 Wallace, J. B., J. R. Webster, and W. R. Woodall (1977), The role of filter feeders in flow-
784 ing waters, *Archiv für Hydrobiologie*, 79, 506–532.

785 Wen, H., and L. Li (2018), An upscaled rate law for mineral dissolution in heterogeneous
786 media: the role of time and length scales, *Geochimica et Cosmochimica Acta*, 235, 1–
787 20, doi:10.1016/j.gca.2018.04.024.